

THE DESIGN AND CONSTRUCTION OF A
BETA-RAY SPECTROMETER

by

GEORGE PEARSON MELLOR

B. A., Colorado College, 1947

A THESIS

submitted in partial fulfillment of the

requirements for the degree

MASTER OF SCIENCE

Department of Physics

KANSAS STATE COLLEGE
OF AGRICULTURE AND APPLIED SCIENCE

1953

Docu-
ment
LO
2668
T4
1953
m4
C.2

To

EUSTACE VIVIAN FLOYD

Gentleman, Scholar, and Master Craftsman

FOREWORD

The research efforts of the author have been devoted predominantly to assorted problems in design, construction, and operational technique associated with Beta-ray Spectroscopy. It is the intent of this thesis to present an account emphasizing several phases of the instrumental and operational history of the project rather than the detailed analytic study of a specific spectrometric problem.

TABLE OF CONTENTS

INTRODUCTION	Page 1
INSTRUMENTATION	4
General Properties of the Beta-ray Spectrometer	4
Details of the Spectrometer Components	7
The Magnet	7
The Evacuation System	8
The Gas Filling System	10
The Camera	12
Source Assemblies	17
Focusing Geometry	20
The Detector	21
Electrification	28
Detector Driving Gear	28
Angular Correlation Provisions	29
Auxiliary Equipment	33
APPLICATION	37
Investigation of the Internal Conversion Electron Spectrum of Tantalum	37
Calibration of the Instrument	37
Survey of a High Energy Region of Ta ¹⁸¹	37
Correction of the Data	40
Interpretation of the Data	40
Appraisal of the Investigation	43
ACKNOWLEDGMENTS	44
LITERATURE CITED	45

LIST OF ILLUSTRATIONS

PLATE I.	Photograph of the Complete Beta-ray Spectrometer	6
Fig. 1.	Schematic Diagram of the Gas Filling System.	11
PLATE II.	Photograph of the Beta-ray Spectrometer Camera.	14
PLATE III.	Construction Diagram of the Spectrometer Camera.	16
PLATE IV.	Construction Diagrams of the Source Assemblies.	19
PLATE V.	Photograph of some Camera Components and Accessories.	23
PLATE VI.	Construction Diagram of the Detector.	26
Fig. 2.	Geiger-Müller Tube Performance Characteristic Curve.	27
PLATE VII.	Photographs of Angular Correlation Features.	32
PLATE VIII.	Photographs of the Semi-micro Drybox.	35
PLATE IX.	A High Energy Region of the Tantalum Spectrum.	39
Fig. 3.	Activity Time-normalization Curve for Ta ¹⁸¹ .	41
Fig. 4.	Corrected Tantalum Spectrum.	42

INTRODUCTION

In contributing to the fund of experimental information supporting the theory of nuclear constitution, Beta-ray Spectroscopy analyzes electronic events which are of nuclear origin or provocation.

When a nucleus suffers a change in quantum state through a reduction in the net energy of the nuclear constituents, the forfeited energy must be dissipated through some transport mechanism. The surplus energy may manifest itself as an emitted gamma-ray having a photon energy equivalent to the corresponding change in nuclear quantum state. Of more mensurable interest however, is a competitive mode of nuclear decay known as Internal Conversion. Here the condemned nuclear energy provokes the ejection of an extranuclear orbital electron, and so happily provides a tangible signal possessing mass and charge, and differing from an ordinary electron in its genesis only. Then the sum of the kinetic energy of this internally converted electron and the binding energy characterizing the orbit of the electron's extranuclear origin exactly accounts for the energy of the initiative nuclear transition.

Extranuclear orbital binding energies for most of the elements are well known from other experimental sources (3). The spectrometric problem now reduces to the measurement of the kinetic energies of the appropriate internal conversion electrons. To approach this problem consider the following argument:

When an electron enters a magnetic field with a velocity

component normal to the field, an electro-magnetic reaction ensues whereby the electron is accelerated in a direction mutually perpendicular to its velocity component and the magnetic field. These ballistical conditions cause the electron to describe a circular trajectory. According to electrodynamics the equation of motion governing this action has the form:

$$(1) \quad f = m \frac{dv}{dt} = Bev^1$$

where: f - central force in dynes acting upon the electron

B - magnetic field intensity in gaussses

e - electronic charge in e. m. u.

v - velocity of the electron in cm./sec.

m - dynamic mass of the electron in grams

$$\frac{m_0}{(1 - v^2/c^2)^{\frac{1}{2}}}$$

where: m_0 - rest mass of the electron in grams

c - velocity of light in cm./sec.

But also according to the mechanics of centrally accelerated particles:

$$(2) \quad f = m \frac{v^2}{\rho}$$

where: ρ - radius of curvature of the particle's orbit in cm.

Combining equations (1) and (2):

$$Bev = m \frac{v^2}{\rho}$$

whence:

$$B\rho = \frac{mv}{e}$$

¹Strictly, $f = d/dt(mv) = Bev$; but since f is perpendicular to v , acceleration of the electron is directionwise only and no work is done. Thus with m constant (for constant v) the expression assumes the above Newtonian form.

This simple working formula reveals that the momentum per electronic charge is curiously equal to the product of the magnetic field intensity in gauss and the radius of curvature of the electron trajectory in centimeters. If a uniform magnetic field is adjusted to a value suitable to the focusing range of a given spectrum and then remains constant, running values of ρ for consecutive monoenergetic electron groups can be measured directly by a spectrometer. Kinetic energies of the monoenergetic electron groups can then be calculated in terms of their respective momenta, $B\rho$ by means of the relativistic formula:

$$E = -m_0c^2 + \left[(m_0c^2)^2 + \left(\frac{3B\rho}{10^4} \right)^2 \right]^{1/2}$$

For electrons with energies in Mev, this formula reduces approximately to:

$$E = -0.511 + \left[(0.511)^2 + \left(\frac{3B\rho}{10^4} \right)^2 \right]^{1/2}$$

INSTRUMENTATION

General Properties of the Beta-ray Spectrometer

Conspicuously curious are the extremes in magnitude existing between the subject and the implement of Beta-ray Spectrometry. For although the electron is one of the smallest characters in our concept of material nature ($m_0 = 9.11 \times 10^{-28}$ gm.), the instrument required to measure the electron's momentum, i.e. the beta-ray spectrometer concerned in this text, incorporates over two tons of coherent apparatus.

The beta-ray spectrometer herein described was of the Fixed-Field, 180° -Focusing Type. Use of constant magnetic fields required that the spectrometer be designed to measure variable values of the momentum parameter ρ . Spectrometers of this type are thus essentially distance measuring devices.

By allowing the electron trajectories to circumscribe approximately 180° arcs, a geometrically inherent focusing property permits the detector to intercept, with negligible loss in energy resolution, a reconverged extended beam of monoenergetic electrons having a small but finite range in angle of departure from the radioactive source. The advantage of collecting a reconverged bundle (rather than a narrow pencil) of monoenergetic electrons is realized as greater signal intensity at the detector for any given ρ .

EXPLANATION OF PLATE I

Photograph of the Complete Beta-ray Spectrometer.

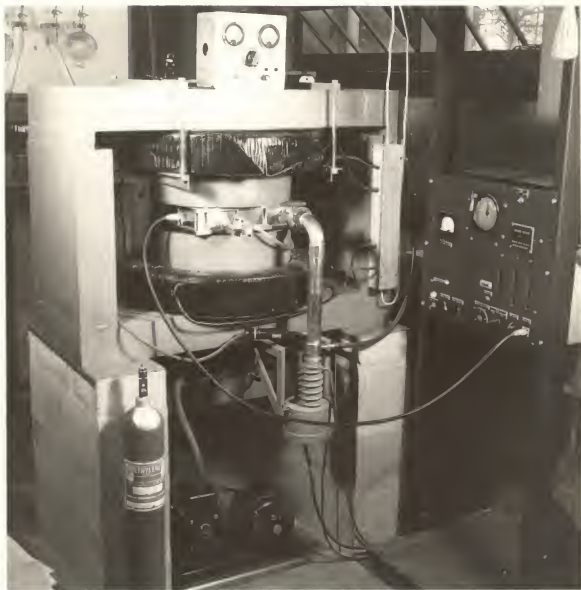
Also shown:

Right: High voltage power supply and decade pulse scaling unit for the detector; channeled to the camera through a coaxial cable.

Atop magnet: Meter and control box for the vacuum thermocouple gauge.

Before the left magnet pier: High pressure cylinder containing gas for recharging the detector-gas reservoir (not present at the time the photograph was taken).

PLATE I



Details of the Spectrometer Components

The Magnet. Electron focusing was effected by a large semi-permanent magnet. Views of this magnet appear in PLATES I and VII. Exclusive of excitation coils, the ferrous portion of the magnet weighs approximately 2,850 pounds.

Two cylindrical, soft iron poles were supported and magnetically linked by a heavy box-shaped yoke made of boiler plate steel. The cylinder dimensions were 16" diameter x 5.5" height. Outside rectangular dimensions of the yoke were 16" x 27.5" x 40". Each pole was anchored to its supporting yoke plate by a single, 1" diameter steel center-bolt. Spaced between each pole was a battery of 80 symmetrically arranged Alnico cylinders (1" diameter x 3" height). These Alnico sub-magnets were concealed by the two large excitation coils which encircle the anchored ends of the poles. The polished pole faces were plane-parallel (to within 0.002") and separated by a 7.65 cm. air gap. Removable steel shims inserted between the vertical yoke pieces and the upper yoke plate make it possible to adjust the pole gap for size and parallelism.

Each excitation coil consisted of approximately 300 turns of #6 copper wire, insulated with shellac and paper, and wrapped round-about with friction tape. The lower coil rested directly upon the lower yoke plate, while the upper coil was suspended from the upper yoke plate by means of two brass brackets. Wherever practicable, appendages to the magnet were constructed of brass or other non-ferrous materials so as to preserve magnetic symmetry.

Magnetization and demagnetization were accomplished by exciting the coils with direct current from a motorgenerator unit. Field intensities of the order of 550 gauss were obtained by brief excitation with currents of about 35 amperes. The soft iron composition of the magnet facilitated the changes in field. Once a desired field had been approximated (as indicated by a gaussometer) excitation was ceased and the field was allowed to stabilize for a few days. Permanent field retention was effected by the 160 aforementioned Alnico sub-magnets.

Calibration of the field was achieved by measuring the value of ρ for a well defined standard "line"¹ of known energy. The field intensity B , was then calculated from the $B\rho$ product corresponding to the known "line" energy. The energies of a number of lines originating from several easily obtained radioactivities have been accurately determined recently by DuMond and collaborators (4).

The Evacuation System. The purpose of the evacuation system is at least fourfold. The air pressure within the camera must be greatly reduced so as to reduce electron scattering and extend the mean-free-path of the electrons sufficiently to allow an adequate proportion of them to reach the detector directly. Low pressure is necessary in order to prevent high voltage breakdown of the electrical elements within the camera. Reduced pressure protects

¹The word "line" refers to a characteristic dark line appearing on the photographic spectrogram of a discrete electron spectrum. Calibration spectrograms were obtained from two simple, box-shaped spectrographs which were designed for use in this magnet.

the delicate detector window from rupture. The detector and the gas filling system must be emptied of air, water, vapor, and any volatile compounds prior to filling them with detector gas as insurance against gas contamination.

Evacuation was accomplished in two stages. The bulk of the air was removed from the system by a rotary vacuum pump (Welch Co., Model #126). Primary evacuation was allowed to proceed until the pressure was reduced to 100 microns or less. Second stage evacuation was then accomplished by a 200 watt, electrically heated oil diffusion pump (Distillation Products Industries, Model #VME 20-01). Normal operating pressures were 1 micron or less.

The rotary vacuum pump rested on the floor between the two concrete piers which supported the magnet, and was connected to the exhaust barrel of the diffusion pump by rubber vacuum hose. Through a flexible mounting the diffusion pump was suspended between two brazed angle-iron brackets which were bolted to the bottom side of the magnet yoke. The high-vacuum barrel of the diffusion pump was soldered to a 1.5" diameter copper manifold which coupled directly to the evacuation port flange of the camera. A rubber gasket was included between the camera and manifold flanges. Flexibility in the diffusion pump mounting permitted the manifold to be swung clear of the camera during the installation or removal of the camera, thus diminishing the danger of straining the soldered manifold joints.

Gross pressure differentials (in the order of 1 mm.) were indicated by a mercury manometer which was mounted at one end of

the spectrometer and connected to the manifold. Higher vacua were measured by a commercial vacuum thermocouple gauge which was screwed into the manifold.

The Gas Filling System. Gas for the Geiger-Müller detector tube (to be discussed later) was mixed and stored in an independent reservoir which was mounted in a wooden cradle atop the magnet. This reservoir was made from a 0.5 liter "pyrex" florence flask sealed at the neck. Commercial gas could be transferred from high-pressure cylinders to the reservoir through a short section of rubber hose which connected the reservoir refill stem to the butterfly valve of the high-pressure cylinder.

The gas mixture most commonly used consisted of 90% argon (as the ion vehicle) and 10% ethylene (as the quencher). The detector tube was usually filled to a pressure of 10 cm. of this gas.

Elements of the gas filling system are shown schematically in Fig. 1., on the following page.

An examination of the stopcock arrangement shown in Fig. 1 explains how the one manometer can be channeled so as to serve independently either the vacuum manifold, the detector, the gas refill line, or the gas reservoir. Although the situation of a double stopcock between the reservoir and the detector necessitated that the detector tube be filled in two stages via the manometer line, it did insure that the delicate Geiger-Müller tube window could not be subjected suddenly to the full gas pressure within the reservoir.

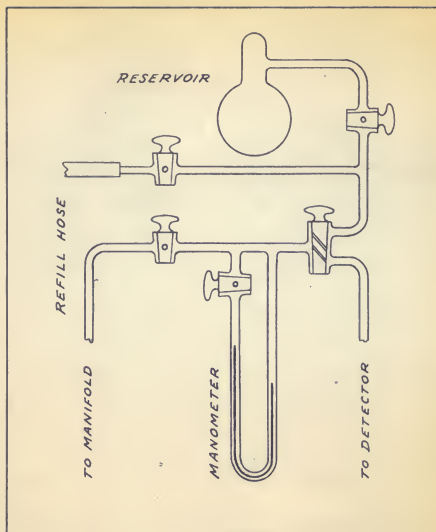


Fig. 1. Schematic Diagram of the Gas Filling System.

The Camera. Basically the functions of the beta-ray spectrometer camera are to provide a low-pressure region of known geometry in which electrons can be focused, and to incorporate some device for detecting the focused electrons.

Since the evacuated camera must withstand atmospheric pressure and also must not by its own presence perturb the magnetic field in which it operates, it is mandatory that the camera be built of some rigid, nonferrous material. Ideally suited to these and other requirements is brass. Thus the camera was constructed almost entirely of brass. Exclusive of lead shielding, which varied in amount - depending upon the radiation characteristics of the sample under study - the camera weighed 55 pounds. The size and configuration of the camera and its components can be ascertained by consulting PLATES II and III. The radical design of the instrument (in particular the semi-circular bay window) will be accounted for under the subtopic, Angular Correlation Provisions.

The camera shell, consisting of a base, five vertical walls, and a lid was fashioned from $\frac{3}{8}$ " brass plate. The walls and base were bolted together with #8-32 screws and the seams sealed with soft solder. During operation the lid (shown in Fig. 1, PLATE VII) was secured by twelve $\frac{1}{4}$ " brass bolts (shown in PLATE V) which screwed into the base, and one short bolt which screwed into a bracket which reinforced the joint between the two oblique front walls. The vacuum seal was provided by a rubber gasket situated between the lid and walls. All areas of the camera interior which were optically accessible to the

EXPLANATION OF PLATE II

Photograph of the Beta-ray Spectrometer Camera.

The camera lid has been removed so as to expose the interior structure. The lucite source assembly, which fits between the floor and ceiling of the bay window, is shown half-withdrawn from its normal operating position.

PLATE II



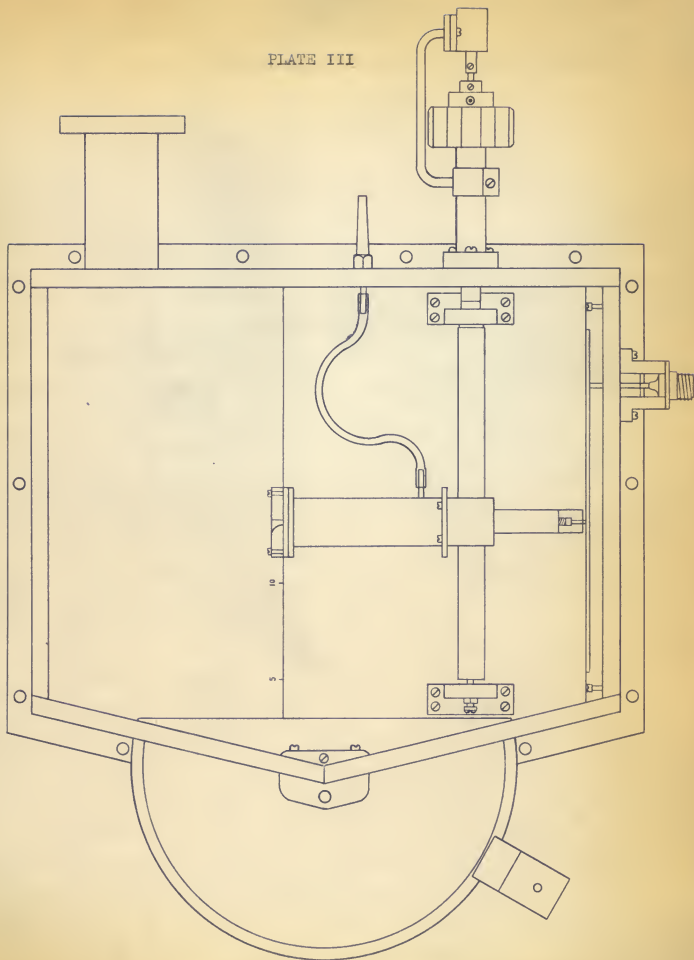
EXPLANATION OF PLATE III

Construction Diagram of the Spectrometer Camera.

Top view, lid removed.

Scale: Approximately $\frac{1}{2}$ actual size.

PLATE III



detector window were lined with thin sheets of electron-absorbing celluloid as a precaution against spurious electron emission from the metallic surfaces.

A flanged exhaust port was silver-soldered to the rear wall of the camera. This port consisted of a section of brass pipe (3.3 cm. I.D.) silver-soldered to a flange containing six #10-32 tapped holes which were aligned with the holes in the evacuation manifold flange. The silver-soldered joints were stepped so as to provide a greater bonding surface at these points of likely stress.

Source Assemblies. For internal conversion electron studies the radioactive sample was normally applied to the adhesive side of a narrow strip of "Scotch" tape. The activated strip was then taped to an aluminum source frame (Fig. 2, PLATE IV). The source frame was then screwed to a brass source tray onto which could be mounted either of two types of focusing slits (Figs. 1 and 5, PLATE IV). This source tray slid into the correct operating position between guides which were located inside the camera's bay window. The gap width of the lucite focusing slit shown in Fig. 1, PLATE IV could be adjusted by means of screws and slotted slit gates. Views of the adjustable focusing slit also appear in PLATES II and V.

For photoelectric studies¹ the radioactive sample was sealed

¹For nuclear transitions having low internal conversion coefficients it is often desirable to measure the gamma-radiations via the mechanism of photoelectric effect. This requires that the radioactive source be covered by a photoelectron source (the radiator) of known Z number. Gamma-ray energies are then represented by $E_\gamma = E_k + B.E.$, where $B.E.$ is the binding energy of the electron ejected from the radiator.

EXPLANATION OF PLATE IV

Construction Diagrams of the Source Assemblies.

Fig. 1. Top view of the source tray mounted with the adjustable lucite focusing slit (actual size).

Triangle $s d 2\rho$ is a two-dimensional representation of the electron focusing geometry. The line s , marks the direction of zero-departure-angle for emissions from the source.

Fig. 2. Aluminum source frame mounted with a "Scotch" tape source strip (actual size). The source frame can be screwed to the middle of the source tray through the two holes shown in Fig. 1.

Fig. 3. Structure of the plastic source envelope (~ 3 times actual size).

Fig. 4. Enlarged top view of the adjustable lucite source holder (~ 3 times actual size).

Fig. 5. Top view of the source tray mounted with the plastic, fixed, focusing slit (actual size). When used for angular correlation studies, the adjustable source holder here included would be replaced by a "backless" source frame.

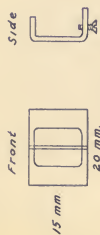


Fig. 2

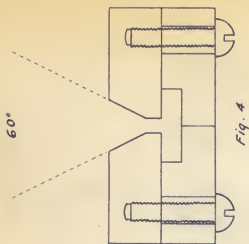


Fig. 4

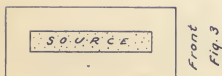


Fig. 3

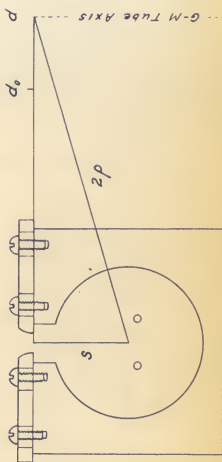


Fig. 1

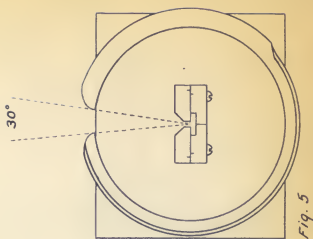


Fig. 5

in a small envelope made of "Scotch" tape and celluloid (Fig. 3, PLATE IV). This envelope, together with an appropriate photo-electric radiator strip, was deposited in the small radiation cavity of the lucite source holder shown in Figs. 4 and 5, PLATE IV. The gate of the source holder was adjustable so that the effective source width could be varied over a small range. The source holder was screwed to the source tray through the same holes which would otherwise accommodate the aforementioned source frame. The enveloped source offered the advantages of safe handling and interchangeability with different radiator strips without fear of contamination.

Focusing Geometry. When the source tray resided in the proper operating position within the camera, the axis of the radioactive source was colinear with the line of intersection of the interior faces of the two oblique front camera walls (PLATE III).

The focal plane, containing the planes of the focusing slit and detector slit, was at a distance, $s=2.54$ cm. away from the plane of the source. For referencing convenience a physical focal line was scribed into the base of the camera and calibrated at the 5 and 10 cm. distances from its intersection with the source line s . With reference to the focusing geometry represented in Fig. 1, PLATE IV, the radii of curvature of the electron trajectories ρ , were calculated in terms of spindle revolutions S , (the spindle will be explained under the subtopic Detector Driving Gear) by means of the following Pythagorean analysis:

s - \perp distance between the source and the focal line.

d - distance along the focal line between the source line s , and the G-M tube axis.

d_o - d of minimum tube approach.

S - number of accumulated spindle revolutions from S_o .
 $S_o = 0000.0$ at d_o .

$k = \Delta d / \Delta S$ - ratio of detector traverse to spindle revolutions.

ρ - radius of curvature of the electron trajectory.

$$\begin{aligned} 2\rho &= \sqrt{s^2 + d^2} \\ d &= d_o + kS \\ &= \frac{1}{2} \sqrt{s^2 + (d_o + kS)^2} \end{aligned}$$

For the camera under discussion:

$d_o = 6.60$ cm.

$s = 2.54$ cm.

$k = 0.0907$ cm./rev.

Then:

$$\rho = 0.5 \left[6.45 + (6.60 + 0.0907S)^2 \right]^{1/2}$$

Values of S were read directly from the camera (subtopic, Detector Driving Gear.). From the point d_o and beyond, ρ is practically a linear function of S . Convenient graphs were drawn which yield corresponding ρ values for values of S .

The Detector. Detection of the focused electrons was performed by a traveling end-window Geiger-Müller tube of conventional cylindrical design. The actual size and structure of the G-M tube and its complements are shown in PLATE VI. Other views of the detector appear in PLATES II, III, and V. Typical performance characteristics of the G-M tube are indicated by the graph in Fig. 2.

EXPLANATION OF PLATE V

Photograph of Some Camera Components and Accessories.

Shown in clockwise order:

Source tray mounted with the adjustable focusing slit.

Radial arm extension bar for supporting the external detector tube used in angular correlation studies.

Internal detector and trolley assembly shown partially disassembled.

Rear and forward spindle bearing mounts. Conical thrust bearing shown protruding from the forward mount.

Sample of the brass camera lid bolts.

Special thin, steel, end wrench designed for adjusting the spindle thrust bearing lock-nut.

A lucite Geiger-Müller tube window slit with mounting screws.

PLATE V



The barrel of the G-M tube was made from 1" brass tubing, highly polished on the inside. A brass window flange was soldered to one end of the barrel and a second matching flange¹ (Fig. 2, PLATE VI) fastens tightly over the first by means of eight #4-40 screws. The interfaces of these two flanges were sufficiently polished to permit the thin plastic G-M tube windows to be clamped between them without the use of gaskets or cement. The other end of the tube barrel was closed by a soldered disk which also furnished the lip by which the G-M tube was screwed to the front face of the detector chassis. A tubular anode guide was concentric with the barrel and soldered to the disk; and passed back, through a hole in the chassis, to the trolley assembly. The anode consisted of a short segment of 5 mil tungsten wire spot-welded to a 20 mil tungsten wire lead which was sealed into a glass insulating tube, which in turn, was sealed with hard wax into the anode guide tube. A small glass bead was fused to the tip of the fine anode wire in order to prevent electrical breakdown due to brushing at the sharp edges of the wire.

The G-M tube was filled with gas through a section of "Tygon" plastic hose connected to a filling stem which penetrated the rear camera wall (PLATE III). The filling stem was in turn connected by rubber hose to the gas filling system.

An assortment of G-M tube slits were made by cementing segments of lucite together in the manner shown in Fig. 3, PLATE VI.

¹Unless otherwise specified, it should be assumed by the reader that all camera components were constructed of brass.

EXPLANATION OF PLATE VI

Fig. 1. Construction Diagram of the Detector (actual size).

- a. window flanges.
- b. Geiger-Müller tube barrel.
- c. rear tube disk.
- d. detector chassis.
- e. trolley tube.
- f. trolley electrode.
- g. lucite trolley guide.
- h. chassis spindle hole.
- i. trolley spring tension screw.
- j. trolley tube support stud.
- k. G-M tube support screws.
- l. anode guide.
- m. gas filling port.
- n. glass anode insulator.
- o. tungsten wire anode.
- p. anti-breakdown bead.

Fig. 2. End view of the G-M tube window.

Fig. 3. A G-M window slit showing the seams where the four segments of lucite have been cemented together.

PLATE VI

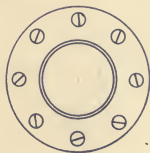


Fig. 2

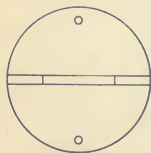
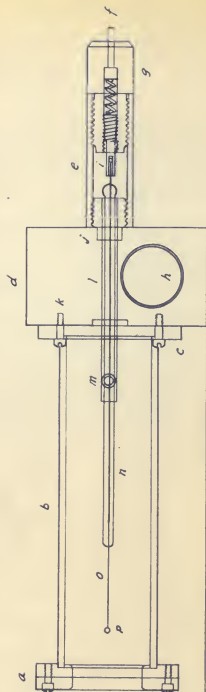


Fig. 3



Camera Base

Fig. 1

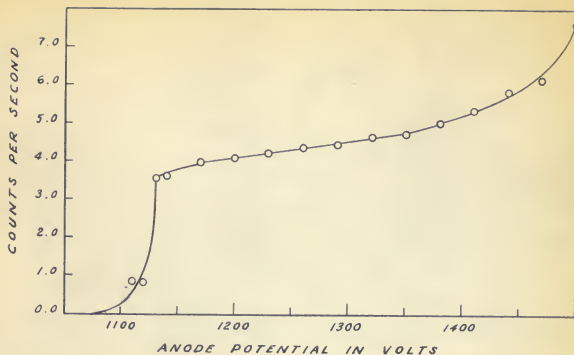


Fig. 2. Geiger-Müller Tube Performance Characteristic Curve.

The tube was filled with a gas mixture of 90% argon-10% $\text{CH}_2=\text{CH}_2$ at a pressure of 10 cm. of Hg. Under these conditions the tube exhibited an approximately linear plateau over a range of 180 volts, with a rise of 10.3% per 100 volts.

The slits were screwed to the outer face window flange (PLATE III).

Electrification. High voltage was supplied to the G-M tube through a trolley assembly which screwed onto the detector chassis. Elements of the trolley assembly and their relations to one another are best described by Fig. 1, PLATE VI. The anode lead made electrical juncture with the trolley electrode through a globule of mercury deposited in a small well in the electrode spring tension screw. The trolley electrode made riding contact with a copper trolley bar which was insulated from the camera wall by a lucite plate. The trolley bar was connected to a commercial exterior coaxial cable coupling by a conductor passing through a lucite plug which was screwed into the right wall of the camera.

Detector Driving Gear. The detector was caused to traverse the focal plane by means of the following machinery. A lathe-threaded, phosphor-bronze spindle (28 threads per inch) passed through a threaded hole in the detector chassis (PLATES II, III, V, and VI). This spindle was supported at both ends by bearing mounts which were screwed to the base of the camera. The forward mount held a conical thrust bearing which was turned from a #10-32 brass screw, and could be adjusted by loosening a lock-nut at the back of the mount. The other end of the spindle was recessed, and passed through a polished bearing hole in the rear mount. Through a split-cylinder arrangement (not visible in the illustrations), the spindle was coupled to a brass spindle-drive shaft and was secured by an "Allen" type set-screw.

A vacuum seal between the drive shaft and the drive shaft-tube was maintained by two commercial "O-ring" type gaskets which fitted into V-shaped grooves cut into the drive shaft.

Spindle revolutions were indicated by a commercial mechanical recorder (Veeder-Root Co.) which was coupled to the drive shaft by a short rod and two set-screws. The recorder was supported by a U-shaped bracket which clamped about the drive-shaft tube. By loosening the bracket ferrule set-screw and the coupling rod set-screw, the recorder could be moved further out from the turning knob if more hand room was desired. The bracket could also be rotated so as to change the reading angle of the recorder. If this latter adjustment were made, care would be taken to return the recorder to its original reading; otherwise, the calibration of the instrument would be invalidated.

Angular Correlation Provisions. With the idea of providing for instrumental versatility, the camera was designed in such a way as to make it adaptable to angular correlation studies - in particular, those of internal conversion electrons with gamma radiation. Internal conversion electrons were detected by the internal G-M tube as described previously, while gamma-rays were detected by an external detector which could be set at various angles with respect to the direction of detectable electron emissions from the source. Angular dependence of coincidence rates between the internal conversion electron and gamma emissions furnishes information about the nuclear spin states and energy levels linked by the radiations.

The external detector was supported by a radial arm which sweeps about a 195° circular bay window which circumspects the radioactive source center at a radius of 10.5 cm. (PLATES II, III, and VII). A 7 mil copper window was soft-soldered to a slotted circular strap which was silver soldered to two $1/8$ " brass plates which formed the floor and ceiling of the bay window assembly. The open end of the assembly fitted into a horizontal slot in the two oblique front camera walls (PLATE II), and the seams were soldered. The radial arm pivoted about a stepped brass bushing which screwed onto the bottom of the camera base. Clearance for the $1/8$ " thick arm was provided by three brass runners which were screwed to the bottom of the base. Additional support was given to the radial arm by an L-shaped brace which rode along the top edge of the bay window strap (best shown in Fig. 1., PLATE VII). When a G-M tube was used as an external detector, the tube was held by an aluminum extension arm which bolted onto the radial arm (PLATES V and VII).

The circular bay window and the circular focusing slit (Fig. 5., PLATE IV) offered a minimum in variation of gamma-ray obstructions about the source.

During angular correlation studies the instrument operated as a coincidence spectrometer. As shown in Fig. 2., PLATE VII, two scaling units monitored the outputs of the two detectors; thence the scaler outputs were channeled to the coincidence circuit. Angular correlation was then observed as the variation of coincidence rates with the angle between the gamma-ray and

EXPLANATION OF PLATE VII

Photographs of Angular Correlation Features.

Fig. 1. View of the camera equipped with an external detector for angular correlation studies. In this case the detector is a commercial G-M tube, mounted in the special aluminum extension bar shown bolted to the primary radial arm.

Fig. 2. View of the instrument arranged to operate as a coincidence spectrometer for angular correlation studies. Top left: commercial scaler channeled to the external detector. Center left: commercial scaler channeled to the internal detector. Bottom left: a coincidence circuit channeled to both scalers.

The two hoses, clamped to the transit panel between the magnet piers (partially visible), are connected to the vacuum manifold and are used to evacuate the two spectrographic cameras.

PLATE VII.



Fig. 1.

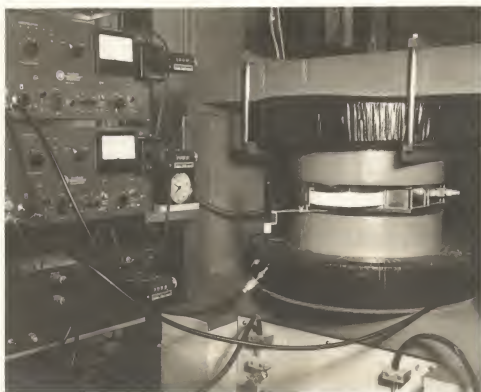


Fig. 2:

electron emissions. This correlation angle was approximately equivalent to the angle subtended by the radial arm and the source line s , (refer to Focusing Geometry for a definition of s).

Auxiliary Equipment

A host of assorted auxiliary instruments and accessories including special tools, jigs, gauges, frames, boxes, Geiger-Müller tubes, slits, shields, sample vials, etc. was designed and manufactured to supplement the central instrument and facilitate various other aspects of the spectroscopic program. These items were too numerous, and in most cases too trivial, to merit individual description. One of these instruments, however is described below.

A semi-micro drybox, the safety device shown in Fig. 1., PLATE VIII, was a miniature drybox designed to confine contamination during the mounting of moderately intense radioactive sources.

The upper section of the cylindrical drybox was a steel turret containing a source-frame clamping stage, a probe port, and two sample-vial holding tubes. The turret could be covered by a thick lucite window which shielded the operator from alpha - and beta - radiation. The lower section of the cylinder fitted onto a wooden base and functioned as a receptacle into which was placed an expendible paper cone. The configuration of the turret elements was such as to permit source spillage to fall freely into the paper cone.

EXPLANATION OF PLATE VIII

Photographs of the Semi-micro Drybox.

- Fig. 1. View of the semi-micro drybox assembled and loaded for use. The lucite window has been removed for the sake of photographic clarity. Pencil suggests the size of the instrument.
- Fig. 2. The semi-micro drybox, partially disassembled.

PLATE VIII



Fig. 1.



Fig. 2.

One vial containing a radioactive sample and another containing a wetting agent were clamped in the turret tubes by means of set-screws; and a blank source strip, mounted on its appropriate frame, was clamped onto the clamping stage. Radioactive sample was transferred from the vial to the strip by means of a glass probe which could be manipulated from the outside through a punctured rubber diaphragm covering the turret probe port.

If the drybox were to become contaminated it could be easily and completely disassembled (Fig. 2., PLATE VIII), thus allowing any contaminated members to be localized and isolated. In an emergency, or in the event that the operator did not wish to take time out to decontaminate, the small drybox could be quickly transferred en toto to an isolation zone.

The main advantage of the semi-micro drybox was the independence and freedom of movement afforded to the operator, who needed not be hampered by cumbersome gloves. Of course the device was by no means a panacea for source-preparing ills as it offered no protection whatever against gamma-radiation and had therefore to be used with dispatch. Further, successful operation of the instrument demanded considerable manual diligence and a rigidly ordered sequence of manipulative moves.

APPLICATION

Investigation of the Internal Conversion Electron Spectrum of Tantalum

Calibration of the Instrument. In order to test the performance of the spectrometer, it was decided to survey a high energy region (in the neighborhood of 0.95 - 1.24 M.e.v.) of the tantalum spectrum. This region was of especial interest since reports in the literature from several independent investigators (2) disclose uncertainties and discrepancies in the K- and L-line energy assignments. In particular the 1.237 M.e.v. K_3 -line (Fig. 4.), reported by Beach, Peacock, and Wilkinson (1), was suspected of containing a weak, unresolved K_4 -line. A preliminary photospectrographic investigation of that K_3 region augmented this suspicion.

Survey of a High Energy Region of Ta.¹⁸¹ A spectrometric survey of the entire 0.95 - 1.24 M.e.v. region was then initiated under the following operating conditions:

source width	~ 1.5 mm.
source height	~ 11.0 mm.
focusing slit width	6.0 mm.
detector slit width	1.6 mm.
internal gamma-ray shielding	~ 10.0 cm. of Pb.

An understanding of the preceeding dimensions can be obtained by refering to PLATE IV.

Results of the survey are presented graphically in PLATE IX. Spectrometric determination of the gamma-ray leakage through the internal lead shielding was made by blocking off electrons at the source with a plate of lucite placed in front of the

EXPLANATION OF PLATE IX

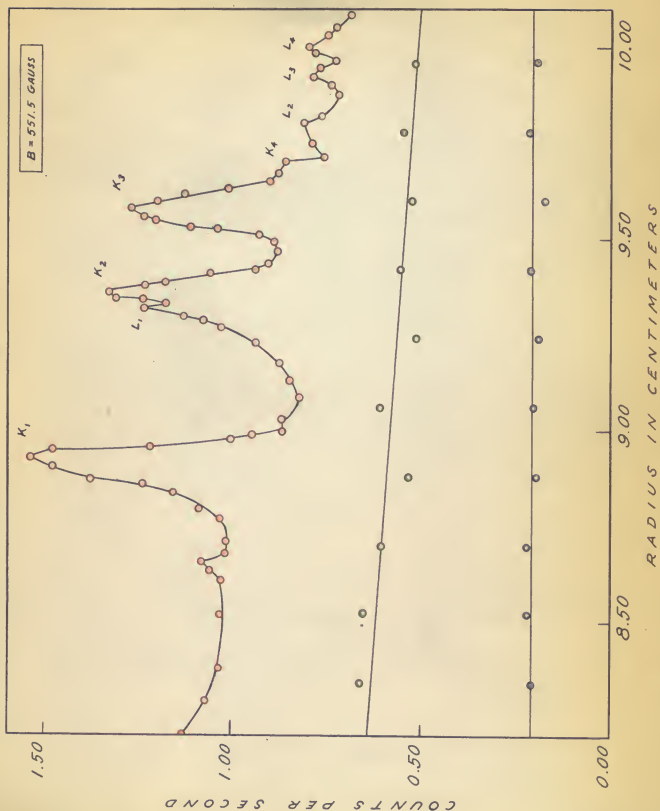
A High Energy Region of the Tantalum Spectrum.

Graphic representation of some internal conversion electron line positions and relative intensities in terms of counting rate vs. radius of electron trajectory .

Key: ● - Composite spectrum.
● - γ - Ray leakage plus background.
● - Background.

TANTALUM SPECTRUM HIGH ENERGY REGION

PLATE IX



focusing slit. The background counting rate (due mainly to cosmic-rays) was spectrometrically evaluated by completely removing the source from the camera.

Correction of the Data. On the basis of a tantalum half-life of 116 days, an activity normalization curve was plotted (Fig. 3.).

Figure 4. is a graph of the corrected tantalum spectrum which results when the spectrum shown in PLATE IX has been time-normalized and deleted of gamma-ray leakage and background contributions. From this representation (Fig. 4.), one can roughly assess the relative line intensities. These give an index of the relative K-shell internal conversion coefficients.

Interpretation of the Data. According to the evidence exhibited in Fig. 4., the suspicion of the existence of a weak K_4 -line appears to have been justified. The line designated as L_4 , however, appears to be too intense (as indicated by its height) to be compatible with the weak K_4 -line. This suggests the speculation that the peak labeled L_4 may actually include another much weaker, unresolved K-line. This same kind of obscurity applies to the L_2 -line which appears to be much too wide — as though it were actually double-peaked.

An obscure, hitherto undetected line unexpectedly appeared in the vicinity of 1.01 M.e.v. (see the peak above $\rho=8.66$ cm., Fig. 4.). This line could very well be an L-line corresponding to a weak K-line previously reported by O'Meara (5). The radiation responsible for this line has not yet been in-

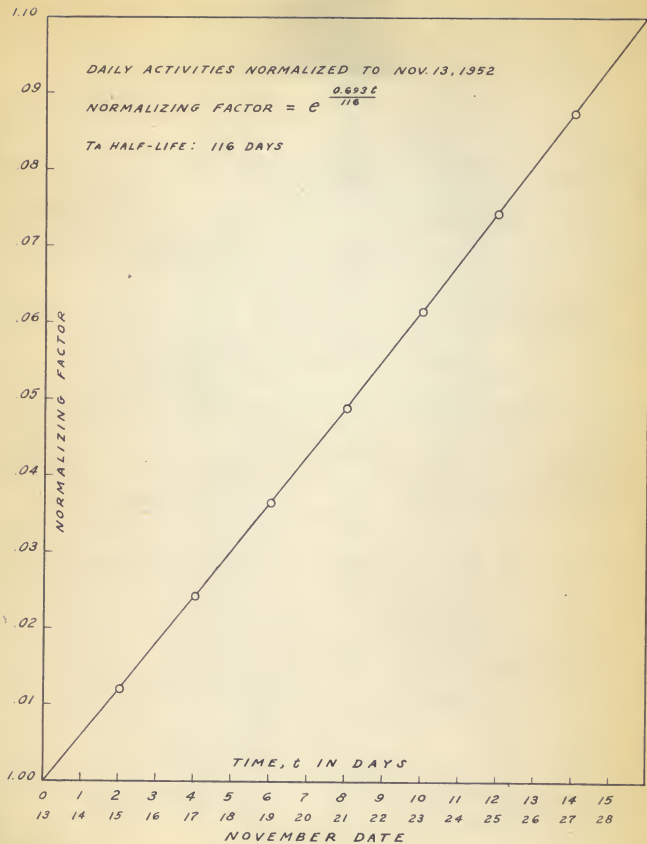


Fig. 3. Activity Time-normalization Curve for Ta.

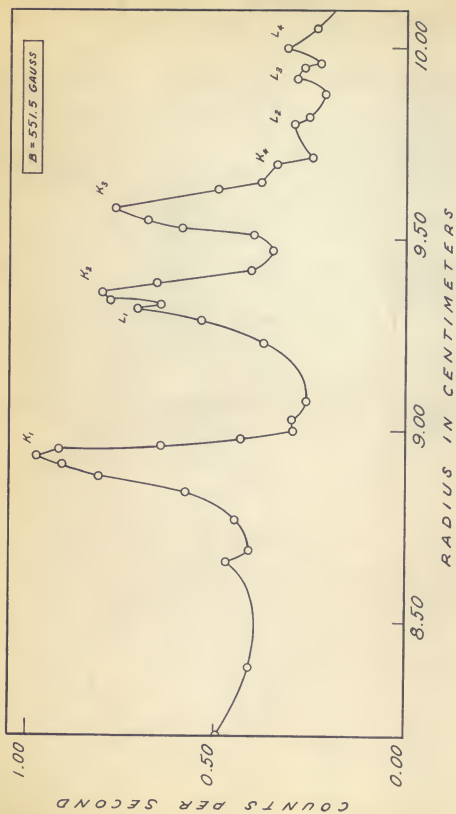


Fig. 4. Corrected Tantalum Spectrum

corporated into any proposed tantalum energy level scheme, and indeed, has not even been reported in the most recent study of the tantalum radiations carried out by DuMond and collaborators (4).

Appraisal of the Investigation

Calculations of the known K-L differences (K_1-L_1 , K_2-L_2 , K_3-L_3) occurring in the spectrum represented in Fig. 4. produced values that were within tolerable limits of those which are expected for internal conversion processes following the $Ta \rightarrow W$ mutation. This evidence, together with the fact that the radioactive sample was obtained from a reliable source (high purity), lends credence to the integrity of the new disclosures as authentic tantalum phenomena.

Although it was not expedient to extend or attempt to refine the spectrometric investigation of the aforementioned uncertainties, the spectrometric results obtained so far, present strong encouragement for a more scrupulous photo-spectrographic investigation of the tantalum high-energy region. Brief spectrographic inquiries to-date have already vindicated some of the above suspicions.

ACKNOWLEDGEMENTS

In recognition and appreciation of their respective contribution to this work, the author gratefully acknowledges the following:

Dr. C. Maxwell Fowler - for his good humored, able, and energetic directorship of this project.

Prof. E. Knight Chapin - for his generous cooperation and advice in photographic matters.

Mr. D. Allan Rittis - for his congenial company and assistance throughout many months of life in the physics shop.

Mr. H. Wesley Kruse - for his contributions to the construction of the spectrometer magnet.

U. S. Atomic Energy Commission - for financing the prolonged research activities of the author.

LITERATURE CITED

- (1) Beach, L. A., C. L. Peacock, and R. G. Wilkinson.
 Gamma-Rays of W¹⁸⁷ in the Low Energy Region.
 Phys. Rev. 75, 211 (1949)

- (2) Cork, J. H., W. J. Childs, C. E. Branyan, W. C. Rutledge,
 and A. E. Stoddard.
 The High Energy Gamma Radiation from Ta¹⁸¹.
 Phys. Rev. 81, 642 (1951)

- (3) Hill, R. D., E. L. Church, and J. W. Mihelich.
 The Determination of Gamma-Ray Energies from Beta-Ray
 Spectroscopy and a Table of Critical X-Ray Absorption
 Energies. R. S. I. 23, 523 (1952)

- (4) Muller, D. E., H. C. Hoyt, D. J. Klein, and J. W. M. DuMond.
 Precision Measurements of Nuclear γ -Ray Wavelengths of
 Ir¹⁹², Ta¹⁸², RaTh, Rn, W¹⁸⁷, Cs¹³⁷, Au¹⁹⁸, and Annihilation
 Radiation. Phys. Rev. 88, 775 (1952)

- (5) O'Meara, F. E.
 Gamma-Spectra of Ta¹⁸² Phys. Rev. 79, 1032 (1950)

THE DESIGN AND CONSTRUCTION OF A
BETA-RAY SPECTROMETER

by

GEORGE PEARSON MELLOR

B. A., Colorado College, 1947

AN ABSTRACT OF A THESIS

submitted in partial fulfillment of the

requirements for the degree

MASTER OF SCIENCE

Department of Physics

KANSAS STATE COLLEGE
OF AGRICULTURE AND APPLIED SCIENCE

1953

Some theoretical considerations which briefly define the problems of Beta-ray Spectroscopy were reviewed.

General properties and features of a 180° -focusing, fixed-field beta-ray spectrometer were explained.

A detailed account of the design, construction, and operational characteristics of the instrument and its components was presented.

Special features, unique to this instrument were described in particular. Camera provisions which make the instrument adaptable to internal conversion electron--gamma ray angular correlation studies were revealed.

An auxilliary instrument, the semi-micro drybox, designed to facilitate the safe handling of radioactive materials during the preparation of spectroscopic sources, was described.

Principally as a test of the performance of the instruments, a portion of the high energy spectrum of tantalum was surveyed and reported. As a by-product of this investigation, a small but significant amount of new information has been added to the knowledge of the tantalum spectrum. The results of the spectrometric analysis were presented in graphic form.